19th Brazilian Congress of Thermal Sciences and Engineering
November 06th-10th, 2022, Bento Gonçalves - RS - Brazil

ENC-2022-0076
STUDY ON CONDENSATION IN POROUS MEDIA EMPLOYING THE LATTICE BOLTZMANN METHOD

Marcelo Adriano Fogiatto
Nathan Mendes
Paulo Cesar Philippi
Pontifical Catholic University of Parana – PUCPR, Imaculada Conceição 1155, 80215-901, Curitiba, Brazil
m.a.fogiatto@gmail.com; nathan.mendes@pucpr.br; philippi@lmpt.ufsc.br

Abstract. *The knowledge of moisture transfer through the building envelope is critically important in the study of building physics, especially when the envelope is made of porous materials. In this case, it may occur condensation in the cavities of the porous media, which may affect the heat, air and moisture (HAM) transfer through the wall. Among the main approaches to simulate this situation, there is the lattice Boltzmann method, which some features, such as the ability to work with complex geometries and the wide availability of multiphase models, are beneficial to this study. Considering a 2-D domain with periodic north-south borders and density defined east and west boundaries at saturated vapor density, as well as the whole fluid domain initially, containing solid bodies, simulations were carried out for different distances between the solids. For a 30 nm distance and reduced temperature of 0.9, the saturated liquid layers around the solids did not reach each other, therefore there was no capillary condensation. On the other hand, for separations of 20 and 10 nm, it occurred. The liquid formation presented different shapes for each distance, and also for different temperatures. An evaluation of the total mass in the domain throughout the time steps was performed to assure the liquid layer growth stopped beyond certain time.*

Keywords: *porous media, lattice Boltzmann method, capillary flows, condensation, multiphase flow.*

1. INTRODUCTION

Throughout the past decades, the efficient use of energy has been a widely covered subject in building physics. Among the main topics, one could mention thermal comfort, efficient use of heat, ventilation and air-conditioning (HVAC) equipment, and the relation between buildings and the microclimate of regions. In these kinds of study, knowledge of HAM transfer through the building envelope is critically important.

Most materials from which the building envelopes are made have a porous structure. In the presence of humidity, water may appear adsorbed at the pore surfaces. When these walls are close, the layers of water from different pore surfaces grow and coalesce, giving rise to capillary condensation in the cavity.

Different methods can be applied in order to study this kind of situation. Between macroscopic and microscopic approaches, we can find the mesoscopic approach. One of the main representatives of this kind of approach is the lattice Boltzmann method (LBM), initially developed by McNamara and Zanetti (1988). The LBM is adequate for this kind of study since it already has a variety of multiphase models available and one of its main advantages is the ability to work with complex geometries. This method has been used in recent years in the study of multiphase flow through porous media (Zakirov and Khramchenkov, 2020; Wang and Peng, 2020; and Farzaneh et al., 2021).

The main purpose of this study is to try to better understand the phenomenon of condensation inside porous structures. For this purpose, we simulate a liquid-vapor system in a two-dimension domain which contains solid bodies, trying to understand the role of pore geometry and temperature on capillary condensation.

2. METHOD AND DOMAIN

The kind of domain considered in this study is represented in Fig. 1. Fluid is present in the white area, surrounding the solid region in blue.

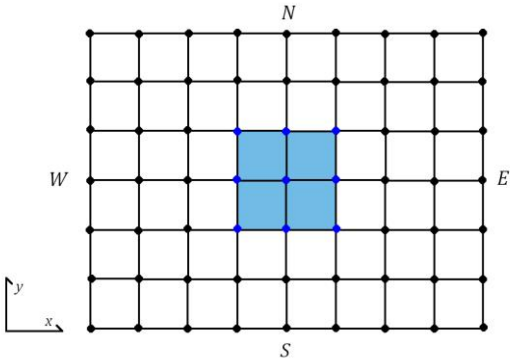

Figure 1. General domain for lattice Boltzmann method

From a general point of view, in the fluid sites, it is simulated the interaction of molecules, such as collision and action of forces between the molecules. In LBM, the modeling of streaming of the so-called distribution function f is also part of the process. When the streaming leads the molecules to the solid area, the half-way bounce back (HWBB) method was applied. It will be looked first into the latter, which depends on the discretization of an advective term. Afterwards, the interaction term Ω, in the form used in this study, will be examined.

Before the discretization process of the advective term, it is necessary to choose a discrete velocity set. In this study, it was chosen the D2V17, developed by Philippi et al. (2006). This velocity set can be seen in Fig. 2.

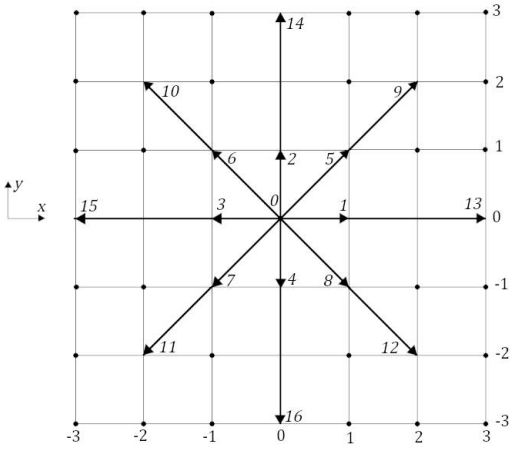

Figure 2. The D2V17 velocity set

The discrete form in space and time of the non-dimensional distribution function $\bar{f}_i$ to each of the 17 directions in this velocity set can be obtained from a Taylor series expansion, as showed in Eq. (1):

$$\bar{f}_i(\vec{x}+\vec{e}_i h, t+\delta) = \bar{f}_i(\vec{x},t) + \frac{d\bar{f}_i}{dt^*} + \frac{1}{2}\frac{d^2\bar{f}_i}{dt^{*,2}} + o\left(\delta^3\right), \tag{1}$$

where $\vec{x}$ is the position vector, $\vec{e}_i$ is the lattice velocity vector, h is the distance between two sites in the lattice, t represents the time, t^* a dimensionless time and δ the time step. Now, assuming the relation regarding the discrete dimensionless interaction term $\bar{\Omega}_i$ in Eqs. (2) and (3) as valid:

$$\frac{d\bar{f}_i}{dt^*} = \bar{\Omega}_i, \tag{2}$$

$$\frac{d^2\bar{f}_i}{dt^{*,2}} = \frac{d\bar{\Omega}_i}{dt^*}, \tag{3}$$

it is possible to perform the Taylor expansion also to the interaction term, and to insert its result into Eq. (1), resulting in Eq. (4):

$$\bar{f}_i(\vec{x}+\vec{e}_i h, t+\delta) = \bar{f}_i(\vec{x},t) + \frac{1}{2}\left[\bar{\Omega}_i(\vec{x}+\vec{e}_i h, t+\delta) + \bar{\Omega}_i(\vec{x},t)\right] . \tag{4}$$

Since Eq. (4) is implicit regarding the interaction term, a change of variables is required before the streaming step, introducing a modified distribution $\tilde{f}_i$ in Eq. (5):

$$\tilde{f}_i = \bar{f}_i - \frac{1}{2}\bar{\Omega}_i . \tag{5}$$

After the streaming step, the original distribution function can be recovered from Eq. (5). With the new values of the distribution function, it is possible to obtain the main macroscopic variables to the lattice sites at each time step, such as the reduced density ρ_r in Eq. (6):

$$\rho_r = \sum_i \bar{f}_i , \tag{6}$$

and the dimensionless macroscopic velocities u_x^* and u_y^* using Eqs. (7) and (8), respectively:

$$u_x^* = \frac{1}{\rho_r}\sum_i \bar{f}_i \, e_{x,i} , \tag{7}$$

$$u_y^* = \frac{1}{\rho_r}\sum_i \bar{f}_i \, e_{y,i} . \tag{8}$$

The discrete interaction term for each direction of the velocity set can be observed in Eq. (9):

$$\bar{\Omega}_i = -\frac{\bar{f}_i - \bar{f}_{eq,i}}{\tau^*} + \left[\frac{1}{\rho_r}\nabla^*\left(\rho_r - A\,P_r\right) + B\,\nabla^*\nabla^{*,2}\rho_r\right].\left(\vec{e}_i - \vec{u}^*\right)\bar{f}_{eq,i} . \tag{9}$$

The first term in the right-hand side of the Eq. (9) is the BGK collision term, as developed by Bhatnagar et al. (1954), where τ^* is the non-dimensional relaxation time, used in this study as a simulation parameter with fixed value of 0.5. The discrete equilibrium distribution $\bar{f}_{eq,i}$, for an isothermal situation, based on the one presented by Siebert et al. (2008), is showed in Eq. (10):

$$\bar{f}_{eq,i} = \rho_r w_i \left[1 + a_s^2\left(\vec{e}_i.\vec{u}^*\right) + \frac{a_s^4}{2}\left(\vec{e}_i.\vec{u}^*\right)^2 - \frac{a_s^2\left(\vec{u}^*\right)^2}{2} + \frac{a_s^6}{6}\left(\vec{e}_i.\vec{u}^*\right)^3 - \frac{a_s^4\left(\vec{u}^*\right)^2}{2}\left(\vec{e}_i.\vec{u}^*\right)\right] , \tag{10}$$

where $\vec{u}^*$ is the dimensionless macroscopic velocity, w_i is the weight factor for each group of directions and a_s is the scaling factor. These latter two are typical to each discrete velocity set and, in the D2V17 case, the values presented by Siebert et al. (2008) are presented in Tab. 1.

Table 1. Weights and scaling factor for D2V17

w_0	0.402005
$w_{1\text{-}4}$	0.116155
$w_{5\text{-}8}$	0.033006
$w_{9\text{-}12}$	0.000079
$w_{13\text{-}16}$	0.000258
a_s	1.643431

The second and last term in the right-hand side of Eq. (9) is the force term, based on the work of Siebert et al. (2014), in which study is presented in detail the discrete forms of the gradient and the gradient of the laplacian for a variable. From a general point of view, the force term used in this study differs from the one in the original work by the choice of

distinct groups of non-dimensional variables. From that equation, P_r is the reduced pressure, and A is the first non-dimensional group, which can be calculated by Eq. (11):

$$A(T)=\frac{P_c}{n_c kT}, \tag{11}$$

where T is the temperature, P_c is the critical pressure, n_c is the critical number density and k represents the Boltzmann constant. The second dimensionless group, B, is presented in Eq. (12):

$$B(T,h)=\frac{\kappa\, n_c}{kTh^2}, \tag{12}$$

where κ is a surface tension parameter, also a function of temperature.

3. RESULTS AND BRIEF DISCUSSION

The first results concern the density profile and the density value of gas and liquid phases of water when the LBM is applied to a 2-D domain with periodic boundary conditions in all sides. In this situation, it was possible to work in a reduced temperature range from 0.75 to 0.96, using the van der Waals equation of state. These density values obtained are the ones used in the main simulations for a given temperature. The density profile obtained for a reduced temperature of 0.9 is presented in Fig. 3.

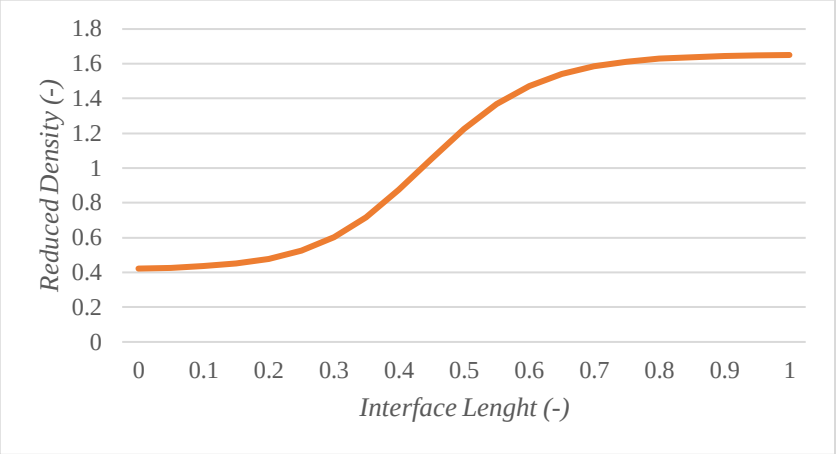

Figure 3. Density profile for reduced temperature of 0.9 obtained by LBM using the van der Waals EOS

In this particular case, the values of density obtained in the LBM simulation do not differ significantly from the theorical values from the van der Waals EOS. Nevertheless, they are the ones used from now on: 0.4161 for saturated vapor and 1.654 for saturated liquid. For lower temperatures and specially for saturated vapor, the values calculated deviate more from those of the EOS, as showed in Tab. 2.

Table 2. Reduced density of saturated vapor from the vdW EOS and from preliminary simulations (h=1.0 nm)

T_r	EOS ρ_r	Simulation ρ_r
0.81	0.254085	0.213086
0.82	0.269243	0.233385
0.83	0.285195	0.253983
0.84	0.302000	0.274965
0.85	0.319729	0.296429
0.86	0.338466	0.318487
0.87	0.358306	0.341377
0.88	0.379366	0.365223
0.89	0.401787	0.390071
0.90	0.425741	0.416150

The following simulations are carried out considering the reduced temperature of 0.9 and h=1.0 nm. The domain of these simulations is a square of 200 x 200 nm filled with fluid, containing two 50 nm solid circles of a different material separated by a channel of fluid. In the first simulation, the separation is 20 nm long.

The initial condition is saturated vapor in all fluid sites of the domain. The north and south boundaries are periodic, while the west and east have defined density. This density is the one of saturated vapor. The macroscopic velocity in these borders is unknown, but will be inwards in the occurrence of condensation around the solids.

The evolution of density values along the time of the simulation can be observed in Fig. 4. In general terms, the blue region represents saturated vapor, the red region is saturated liquid, the white one is the liquid-gas interface and the yellow circles are the solids.

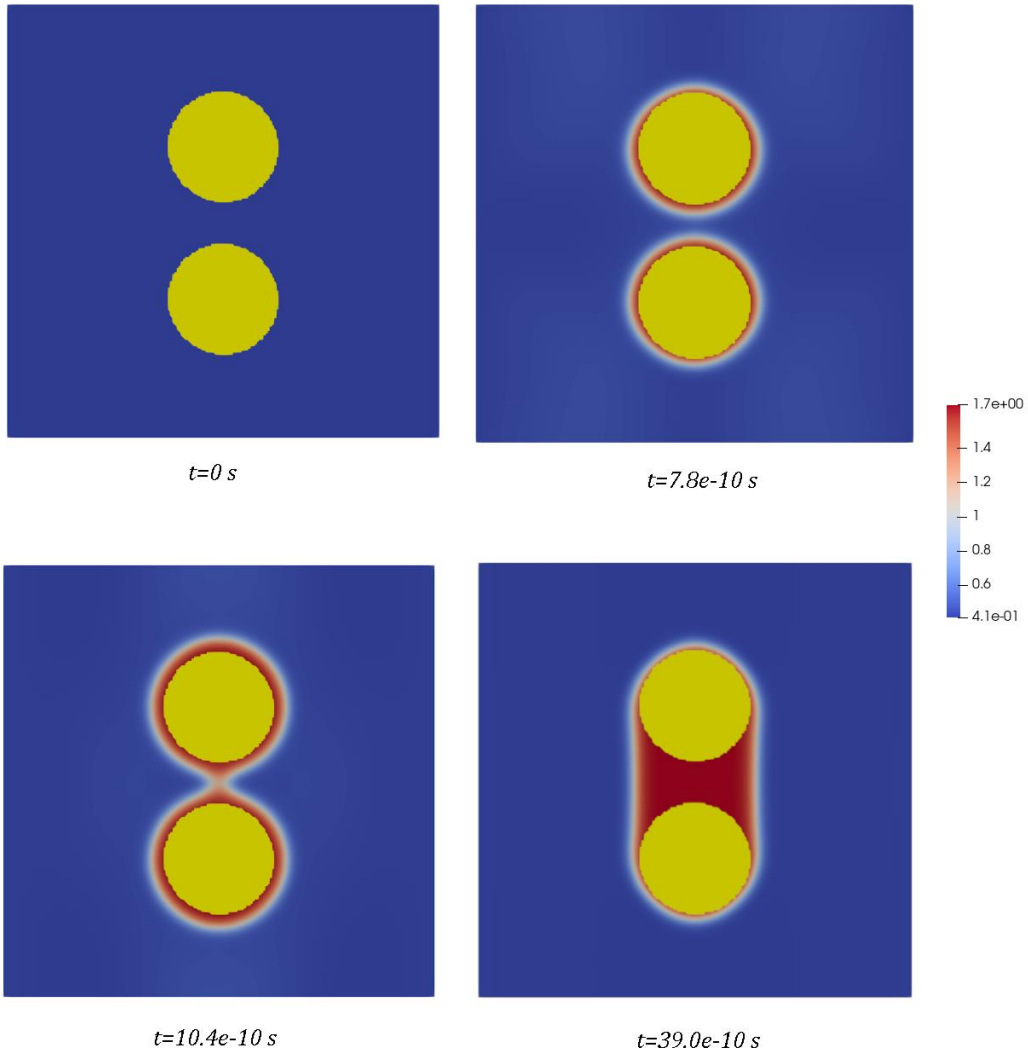

Figure 4. Density results for reduced temperature of 0.9 in 200 x 200 nm domain with 50 nm diameter solids and separation of 20 nm.

It can be observed that a layer of saturated liquid is formed around the solids and, when the liquid layers of the two solids meet, it occurs condensation in the channel. After it, the system tends to an equilibrium state and the liquid region stops to grow. It can be confirmed by the plot of the mass of the system during the time of the simulation, as showed in Fig. 5.

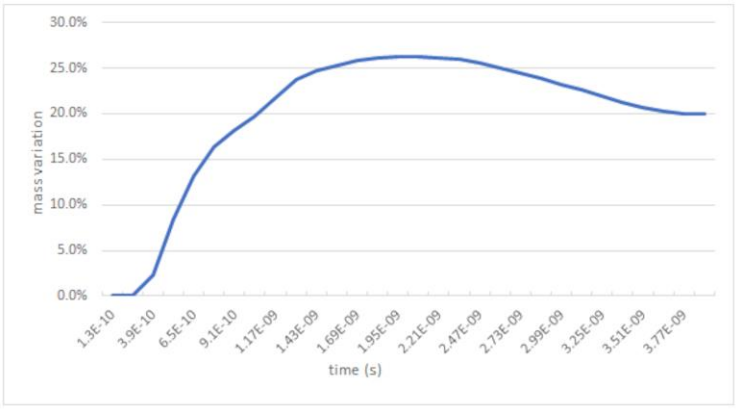

Figure 5. Variation of mass inside the domain along the time.

In this study, the separation length between the solids seems to be also an important factor. With the same time of simulation of the previous one, the calculations were performed for distances of 10 and 30 nm. The final results are seen in Fig. 6.

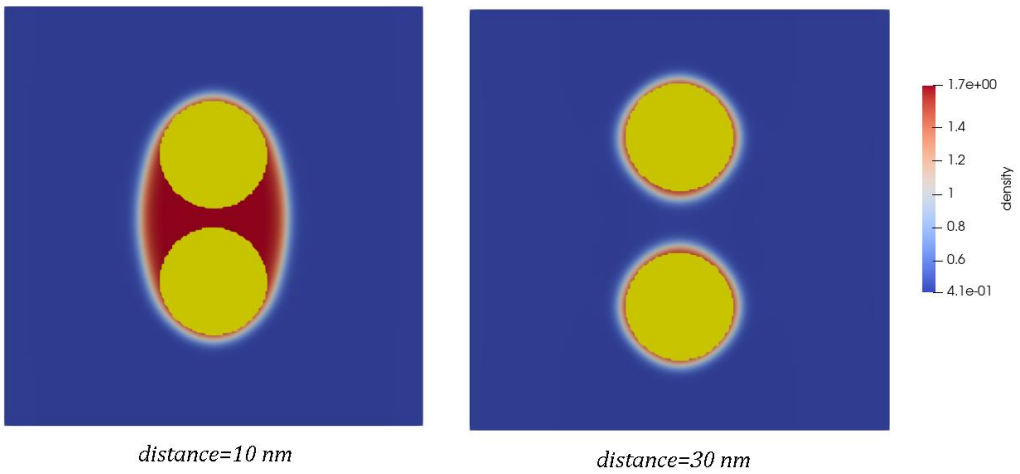

Figure 6. Density results for reduced temperature of 0.9 in 200 x 200 nm domain with 50 nm diameter solids and separations of 10 and 30 nm.

As observed, in the largest separation situation the saturated liquid layers do not touch and, therefore, the condensation in the channel does not occur. On the other hand, with 10 nm distance the condensation regarding the two solids unites, but assumes a different shape of the first situation, like one lump of saturated liquid.

More simulations were carried out in the same conditions as the last, but with a different geometry, in order to evaluate the radius of the interface for different temperatures. It was performed in a 300x300 nm domain, with 100 nm diameter solids separated by a 13 nm channel. It was performed for a reduced temperature range from 0.82 to 0.89. The interface geometry obtained for different temperatures within that range is showed in Fig.7.

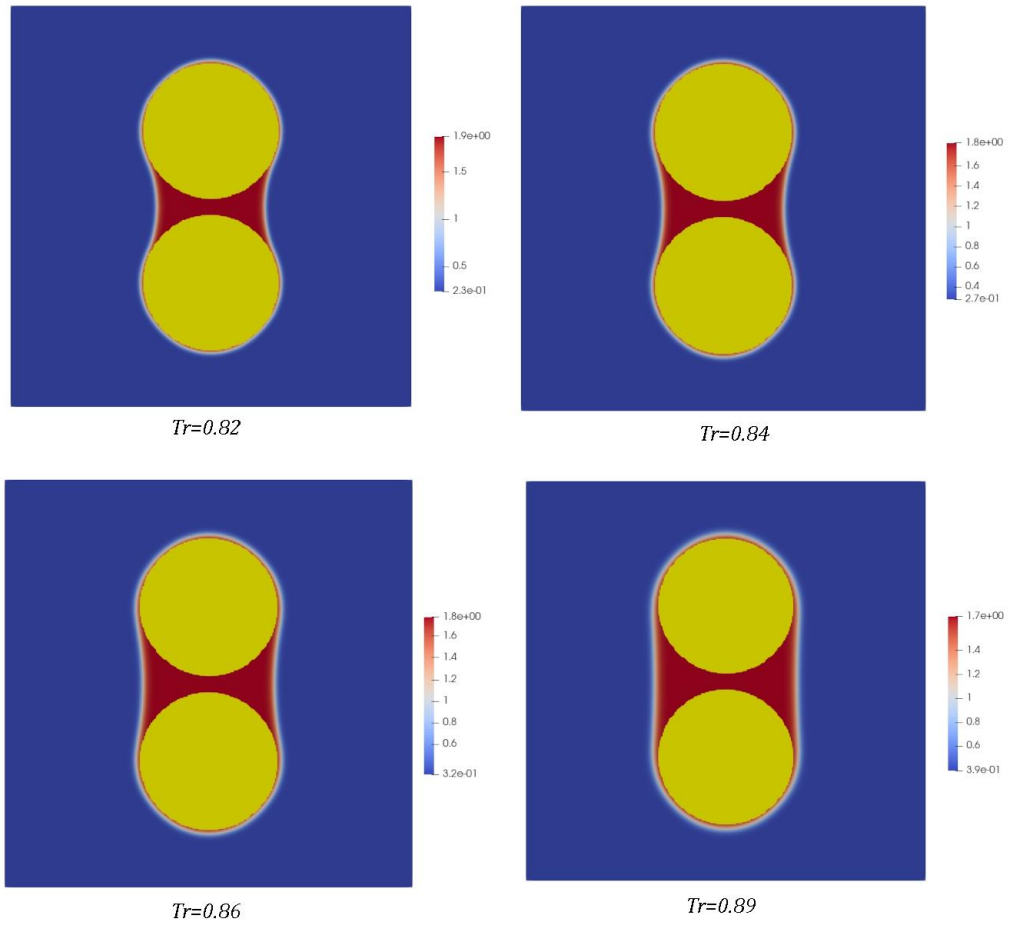

Figure 7. Liquid-vapor interface geometry for different temperatures

The relation between the radius measured for each temperature can be observed in Fig. 8.

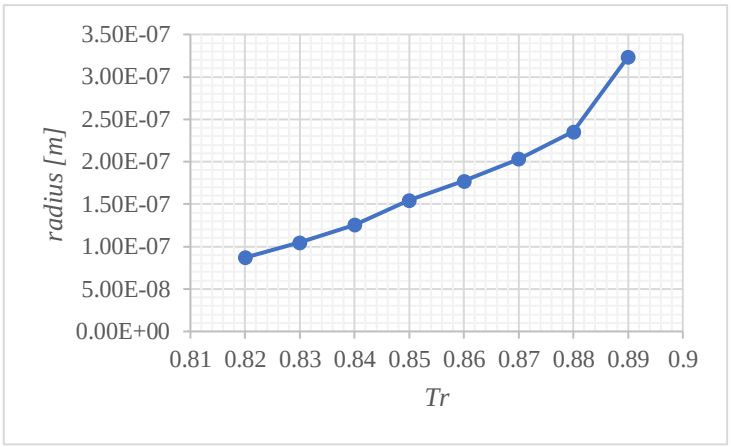

Figure 8. Interface radius for different temperatures

At higher temperatures, the density ratio between the vapor and liquid phases decreases, leading to higher interface radii, as seen for reduced temperature of 0.89 in Fig. 7, where it tends to a limit situation where the interface appears as a straight line. Beyond that, the expected is what occurs in the first item of Fig. 6.

4. CONCLUSION

A study on capillary condensation inside cavities of porous media was carried out using multiphase LBM. It has been showed that the size of the cavity and fluid temperature may influence the occurrence or non-occurrence, besides the

shape of the condensed fluid formation inside the porous medium. Further developments of this model can lead to evaluation of the impact of capillary condensation on the rate of fluid flow through a medium, which can be achieved by setting different values of density at east and west borders.

5. ACKNOWLEDGEMENTS

The authors thank the CAPES – *Coordenação de Aperfeiçoamento de Pessoal de Nível Superior* – of the Ministry of Education of Brazil, Brazilian Council for Research (CNPq) and Pontifical Catholic University of Paraná (PUCPR) for the financial support.

6. REFERENCES

Bhatnagar, P.L., Gross, E.P. and Krook, M., 1954. "A model for collision processes in gases. I. Small amplitude processes in charged and neutral one-component systems". *Physical Review*, Vol. 94, No. 3, pp 511-525.

Farzaneh, M., Ström, H., Zanini, F., Carmignato, S., Sasic, S. and Maggiolo, D., 2021. "Pore-scale transport and two-phase fluid structures in fibrous porous layers: application to fuel cells and beyond". *Transport in Porous Media*, Vol. 136, pp. 245-270.

McNamara, G.R. and Zanetti, G., 1988. "Use of the Boltzmann Equation to simulate a lattice-gas automata". *Physical Review Letters*, Vol. 61, No. 20, pp. 2332-2335.

Philippi, P.C., Hegele Junior, L.A., dos Santos, L.O.E. and Surmas, R., 2006. "From the continuous to the lattice Boltzmann equation: The discretization problem and thermal models". *Physical Review E*, Vol. 73, No. 5, pp. 056702-1-056702-12.

Siebert, D.N., Hegele Junior, L.A. and Philippi, P.C., 2008. "Lattice Boltzmann equation linear stability analysis: thermal and athermal models". *Physical Review E*, Vol. 77, No. 2, pp. 026707-1-026707-9.

Siebert, D.N., Philippi, P.C. and Mattila K.K., 2014. "Consistent lattice Boltzmann equations for phase transitions". *Physical Review E*, Vol. 90, No. 5, pp. 053310-1-053310-15.

Wang, L. and Peng, Z., 2020. "Pressure boundary condition in a multiphase lattice Boltzmann method and its applications on simulations of two-phase flows". *International Journal for Numerical Methods in Fluids*, Vol. 92, No. 7, pp. 669-686.

Zakirov, T.R. and Khramchenkov, M.G., 2020. "Simulation of two-phase fluid flow in the digital model of a pore space of sandstone at different surface tensions". *Journal of Engineering Physics and Thermophysics*, Vol. 93, No. 3, pp. 733-742.

7. RESPONSIBILITY NOTICE

The authors are the only responsible for the printed material included in this paper.